Optik - International Journal for Light and Electron Optics 172 (2018) 295–301

Contents lists available at ScienceDirect

Optik

journal homepage: www.elsevier.com/locate/ijleo

Electronic structure, optical and structural properties of Si, Ni, B and N-doped a carbon nanotube: DFT study

Mustafa Kurban

Department of Electronics and Automation, Ahi Evran University, 40100 Kırşehir, Turkey

ARTICLE INFO

Keywords:
Doped carbon nanotubes
Electronic structure
Bandgap
Refractive index
DFT

ABSTRACT

The electronic structure, structural and optical properties of a carbon nanotube (CNT) and silicon (Si), nickel (Ni), boron (B) and nitrogen (N)-doped CNTs have been investigated by density functional theory (DFT) simulations. We present a comparative analysis to demonstrate how the dopant atoms interact with a CNT. The geometrical properties, lowest harmonic frequency, total energy, dipole moment, Mulliken atomic charges, formation energy, HOMO-LUMO gap, optical refractive index and density of state spectra are analyzed using DFT. The optical absorption spectra are also researched based on TD-DFT method. The bond distances and the corresponding properties exhibit remarkable variations based on the type of the dopant atom. Si and Ni atoms was found to considerably reduce the band gap of CNT. The effect of dopant atoms is quite pronounced in enhancing the electronic and optical absorbance properties of the pure CNT. Our results suggest that a dopant atom has different effect on the pure CNT and it may have potential in designing new electronic devices.

1. Introduction

Carbon nanotubes (CNTs) suggest great promise for future developments in many fields due to their unique and special electrical and structural properties. Hence, considerable achievements have been conducted in the field of the CNTs in the recent years. Although pure CNTs have been of great interest, the use of a dopant atom on pure CNT gives rise to an increase in their abilities for different applications. Therefore, the doping of an atom on the CNTs has become a hot topic recently. According to this viewpoint, doping dopant atoms on the CNTs has become a more effective way for improving the chemical, electrical, optical, mechanical and physical properties of CNTs. For example, a narrower CNT required less energy cost to substitute carbon atom with boron (B) or nitrogen (N) [1]. The conductivity of CNT can also be further enhanced by doping B atoms to CNT for increasing the number of hole-type charge carriers [2]. The dissociation barriers of O_2 and H_2 on CNTs are greatly reduced due to the N-doping [3,4]. Facile oxygen reduction reaction also observed in metal-free N-doped CNTs [5,6]. Nickel (Ni) doped CNTs improved the ability of CNTs to absorb gas molecules [7]. A single NO_2 molecule can also be chemically adsorbed on the outer surface of silicon (Si)-CNT with a relatively large adsorption energy (~1.0 eV), and the electronic properties are modified by the NO_2 adsorption [8]. In addition, Si-doped CNT significantly enhanced the reactivity of CNTs, thus it is a good candidate as a gas sensor or drug delivery device [9,10].

All the mentioned above examples indicate the role of doping an impurity atom on the CNTs and invite further investigation about the electronic, optical and structural properties of the doped system to obtain desirable properties. To our knowledge, there is no any comparative study on Si, Ni, B and N doped a chiral CNT in the literature. Thus, the major aim of this study is to probe and compare the influence of Si, Ni, B and N-doped CNT system on the above mentioned properties of the CNT. On the optimized structures, we

E-mail addresses: mkurbanphys@gmail.com, mkurban@ahievran.edu.tr.

https://doi.org/10.1016/j.ijleo.2018.07.028
Received 10 May 2018; Accepted 9 July 2018

perform B3LYP/ LanL2DZ using density functional theory (DFT) approach to calculate the geometrical properties, lowest harmonic frequency (ω), total energy (E_T), dipole moment (D_{Moment}), Mulliken atomic charges (MAC), formation energy (E_f), HOMO-LUMO gap (E_g), optical refractive index (n) and density of state (DOS) spectra of the CNT, Si, Ni, B and N-doped CNT to gain better understanding of impurity atoms interact with CNT. In addition, optical absorption of four atoms-doped CNT and CNT systems are analyzed with time-dependent (TD)-DFT based on optimized structures.

2. The method of calculations

Geometrical optimizations of the CNT with and without doped atoms were carried out using DFT [11] at the B3LYP level. The exchange term of B3LYP consists of hybrid Hartree–Fock (HF) and local spin density (LSD) exchange functions with Becke's gradient correlation to LSD Exchange [12]. The correlation term of B3LYP consists of the Vosko, Wilk, and Nusair (VWN3) local correlation functional [13] and Lee, Yang, and Parr (LYP) correlation functional [14]. The Los Alamos LanL2DZ split–valence basis set [15–17] has been used in the calculations. The calculations have been performed using the GAUSSIAN09 program package [18]. Hydrogen atoms are placed on the dangling bond at both ends because at chiral ends neighboring dangling bonds can pair-up to form C≡C triple bonds that constitute a considerable stabilization effect [19]. The geometry of the CNTs were optimized without imposing any symmetrical constraints and the lowest total energy configuration was assumed as the global minimum case. The structure is taken as the local minima on potential energy surface having positive vibration frequencies, that is, there is no any transition state for the CNT models. After geometric optimization, TD-DFT method used to analyze optical absorption of the CNT and doped CNT at the CAM-B3LYP [20] level because B3LYP actually underestimates excited-state energies [21–23].

3. Results and discussions

3.1. The structural analysis

Different views of optimized ground state structure of the CNT are showed in Fig. 1. The CNT is a chiral tube with the dimeter and length of 4.89 and 4.67 Å, respectively. The relaxed geometries for the CNT, the Si, Ni, B and N-doped CNTs are shown in Fig. 2, where the geometrical parameters for a selected C atom in the CNT and the Si, Ni, B and atoms in the Si, Ni, B and N-CNTs are given to observe and compare the effect of the Si, Ni, B and N impurity on the CNT structure. It is noted that the bond distances near the impurity atom is severely distorted (see Fig. 2) for Si and Ni-doped CNT, where the impurity Si and Ni projects out of the CNT wall due to their larger size than the C atom. The calculated pyramid solid angle on the Si, Ni and N atoms center is found to be 66.07° (360°–100.39°–93.29°–106.25°), 47.69° (360°–89.36°–110.06°–112.89°) and 23.13° (360°–113.58°–108.49°–114.83°), respectively, however; it on the B atom center is 10° (360°–114.58°–112.50°– 122.92°). It is larger for Si, Ni and B atoms than that on the selected C atom center, 9.4° (360°–100.39°–93.29°– 106.25°) while it is almost the same for B atom comparing with the selected C atom center. These geometrical distortion results in an important change of the electronic property of the CNT.

The vibrational stability of all CNT models is examined on the basis of the vibrational modes. The positive vibrational spectra, that is no any kind of imaginary frequency for the CNT models, are found that the optimized geometry located at stationary point on the potential energy surface. Calculated the lowest vibrational harmonic frequencies for the CNT models are tabulated in Table 1. Seen from the lowest vibrational frequencies, all these structures are more stable than the CNT. Comparing Si, Ni, B and N-doped CNTs, Ni-doped CNTs is found to be the most stable structure (see Table 1).

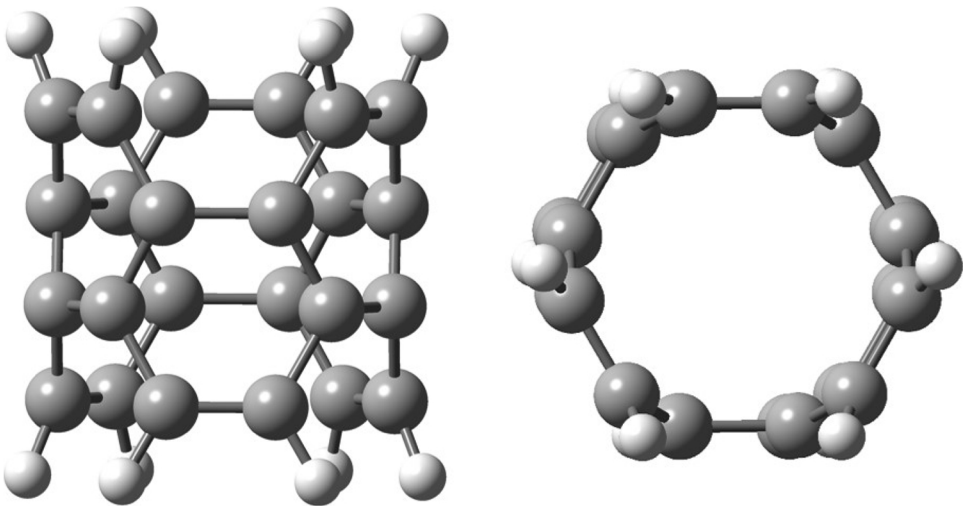

Fig. 1. Different views of the optimized CNT.

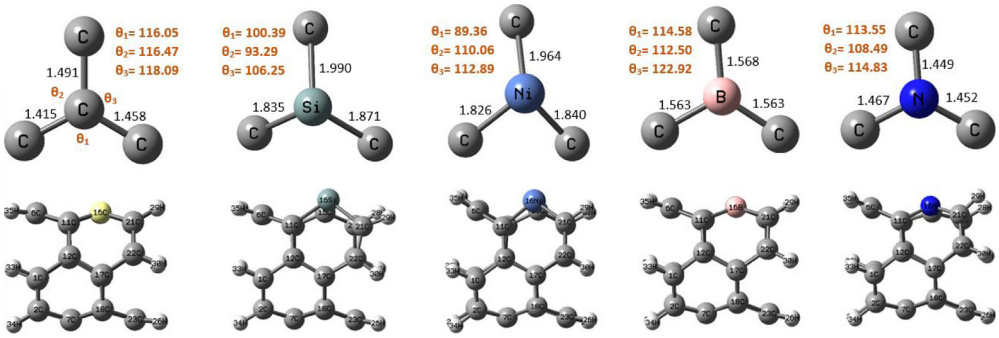

Fig. 2. Optimized structures for the CNT and Si, Ni, B and N-doped CNTs with the geometrical parameters for a selected C atom in the CNT and the Si, Ni, B and N-doped CNTs. The bond lengths are in Å, and the angles are in degrees.

Table 1
The lowest vibrational frequencies (ω, cm^{-1}), total energies (E_{Total}, $a.u.$), HOMO and LUMO energies (E_{HOMO}, E_{LUMO}, eV), HOMO-LUMO gaps (E_{Gap}, eV), dipole moments (D_{Moment}, $Debye$) for the pure CNT and Si, Ni, B and N-doped CNTs.

Property	CNT	Si-CNT	Ni-CNT	B-CNT	N-CNT
ω	143.83	103.56	53.45	123.10	116.85
E_{Total}	−921.3	−887.1	−1052.5	−908.1	−937.9
E_{HOMO}	−4.77	−4.70	−5.07	−4.43	−4.94
E_{LUMO}	−2.42	−2.95	−2.77	-2.32	−2.69
E_{Gap}	2.34	1.75	2.32	2.10	2.24
D_{Moment}	0.00	0.78	0.97	1.41	1.05

3.2. The energetic analysis and relative stability

The total energies (E_T) of the optimized the CNT models are given in Table 1. Comparing the energies in terms of the magnitudes, Ni-CNT is more stable than the other models. Fig. 3 show that the results for the formation energies (E_f) of Si, Ni, B and N-doped CNTs. Using the total energy calculations, E_f can be given,

$$E_f = E[doped{-}CNT] - E[CNT] - E[doped{-}atom] + E[C], \quad (1)$$

where $E[doped{-}CNT]$ is E_T of the atom doped-CNT, and $E[CNT]$ is E_T for the pure CNT. $E[doped{-}atom]$ is $E_T/atom$ in the bulk of doped atom and $E[C]$ is $E_T/atom$ of C in the pure CNT. From Fig. 3, E_f converges to a value of 1.96 eV, which is E_f for N-CNT. From small value of E_f of N-doped CNT, it is found that N-CNT needs a smaller energy cost to substitute a carbon atom with a N atom, while Ni-CNT needs much greater energy (5.79 eV) cost than that of the other CNT models. Moreover, one can conclude that the B and N doping on the CNT become more preferable in energy than Si and Ni-doped CNT.

3.3. Density of states (DOS), HOMO, LUMO and HOMO-LUMO gaps (E_g)

Density of states (DOS) (Fig. 4(a–b)) indicates the HOMO and LUMO levels of the CNT, Si, Ni, B and N-CNT. To see clearly

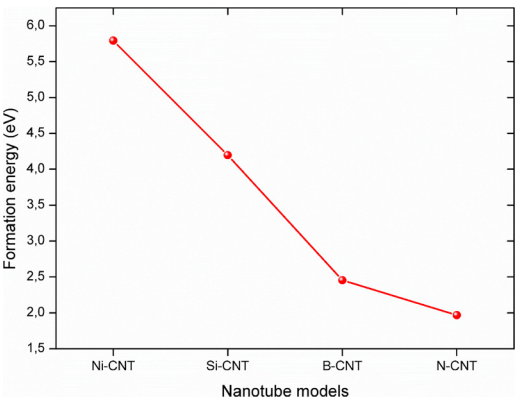

Fig. 3. Formation energy for Si, Ni, B and N-doped CNTs.

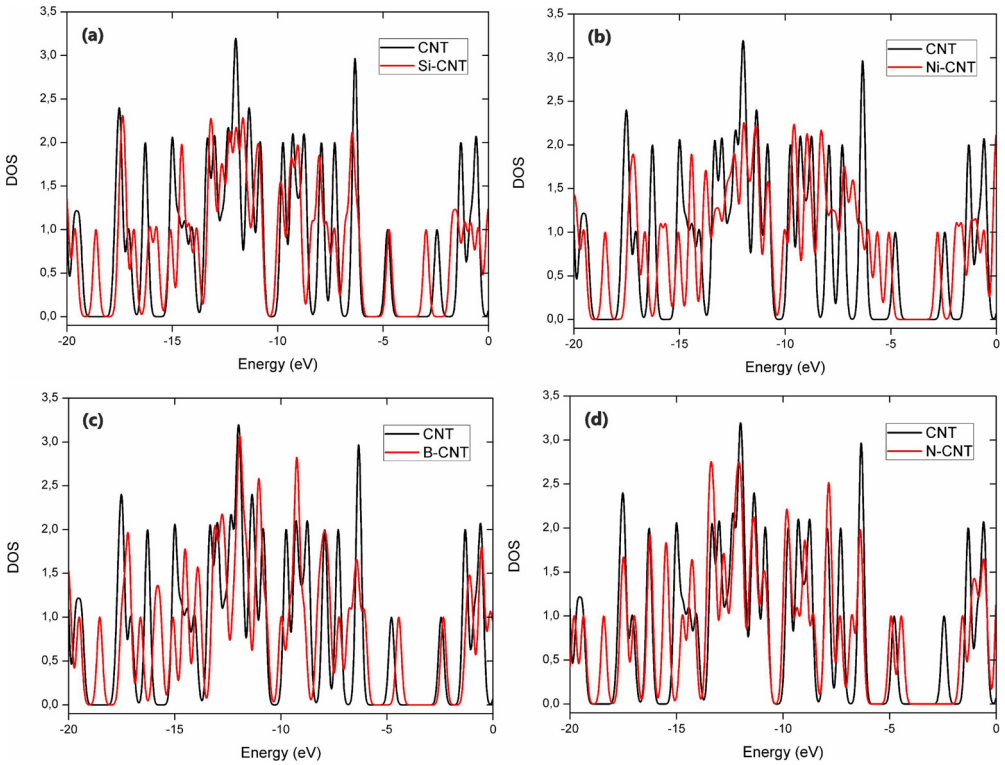

Fig. 4. Density of state (DOS) spectra of (a) Si, (b) Ni, (c) B and (d) N-doped CNT with the CNT obtained Mulliken population analysis.

difference of energy levels between the CNT and doped-CNT, DOS of the CNT is given together on each DOS Figure. From Fig. 4, the HOMO and LUMO levels of the CNT lie at 4.77 and 2.42 eV (Table 1), respectively. Therefore, E_g is about 2.34 eV. The energy of HOMO and LUMO levels of the CNT is lower than Ni and N-doped CNT Similarly, the energy of HOMO levels of Si and B-doped CNT are lower and that of the LUMO is higher than the corresponding value of Si-CNT and lower than the corresponding value of B-CNT. Thus, $E_g$of the CNT is greater than that of Si, Ni, B and N-doped CNT. From Fig. 5, it is shown that for the all doped-models, the Si, Ni, B and N-doping tend to nicely decrease E_g of the pure CNT (from approximately 2.34 eV (the pure CNT) to 1.75 eV (Si-CNT)). Compared with the pure CNT, it is obvious that the doped Si, Ni, B and N atoms contribute to the in E_g. From the results, the electrical conductivity of the all doped models changes considerably with doping of one atom. In addition, Si-CNT with the lowering of the band gaps (1.75 eV) can be preferred for optoelectronic applications or devices, which prefer lower band gaps because the electronic transfer is easier. It implies that E_g for Si-CNT compared to that of the CNT, Ni, B, and N-doped CNT allows easy excitation of electrons from HOMO to LUMO.

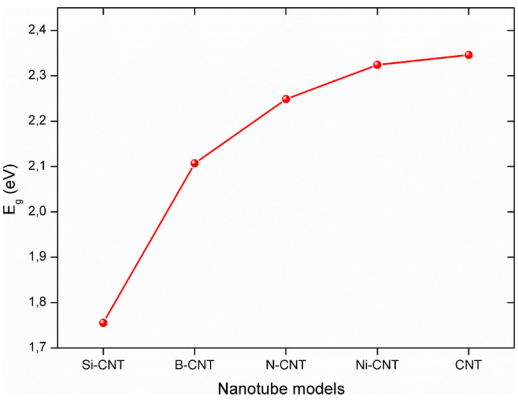

Fig. 5. Variation of the HOMO–LUMO gaps (E_g)of the CNT and Si, Ni, B and N-doped CNTs.

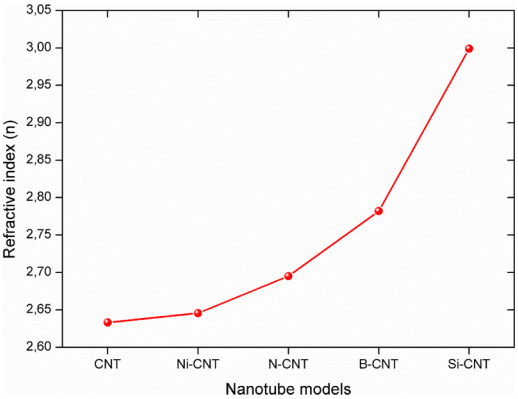

Fig. 6. Optical refractive indices of the CNT, Si, Ni, B and N-doped CNT.

3.4. The optical refractive index (n)

The optical refractive index (n) values of the CNT, Si, Ni, B and N-doped CNT obtained from Ravindra relation [24] which represents a linear relation governing the variation of $n$with E_g is defined as:

$$n = 4.084 - 0.62E_g \tag{2}$$

The relation is used to calculate n, because it is more compatible with experimental results [25]. Fig. 6 shows the optical refractive indices of the CNT, Si, Ni, B and N-doped CNT. The values of n are found to be in orders: Si-CNT (2.99) > B-CNT > (2.78) > N-CNT (2.69) > Ni-CNT (2.64) > the pure CNT (2.63). From Fig. 6, $n$of the CNT models increase from CNT (2.63) to Si-CNT (2.99). These results show that $n$of the CNT can be controlled with Si, Ni, B and N-doped CNT.

3.5. Mulliken atomic charge (MAC) analysis and dipole moment

The charge distribution has a significant role for quantum mechanical applications. The Mulliken atomic charges of the CNT, Si, Ni, B and N-CNT gathered in Table 2. According to Mulliken population analysis, the charge distribution of the CNT depends on the type of dopant atom. The charges of the C atoms of the pure CNT in the same positions show different charge comparing the charges with the doped-CNT. For example, the charge of C11 atom is positive (0.06) in the CNT, however, the value of the charge of the same atom is negative (-0.31) in the Si-CNT. The C16 atom (selected atom for dopant atom) exhibits a positive charge (0.98) the value of the charge for the Si-CNT is bigger than others. Hydrogen atom exhibits a positive charge because it is an acceptor atom. The positive charge (0.06) on the selected carbon atom ranges from -0.29 to 0.98, emphasizes that there exists a rather strong hybridization between the doped Si, Ni, B and N atoms and the neighbor carbon atoms. This is also reflected in dipole moment values which are other important electronic properties. Comparing the values of the dipole moments for the four atom-doped models indicates that the larger dipole moment is evident for the B and N-doped models. This represents the stronger intermolecular interaction. The highest value of component of dipole moment along the z-axis ($\mu_y = -1.2517$ Debye) predicts large opposite charge separation in the B-CNT. The corresponding total dipole moment has been calculated to be 1.4186 Debye.

3.6. UV–vis absorption spectroscopy

We carry out the optical absorption of the CNT, Si, Ni, B and N-doped CNTs (see Fig. 7). Compared with the pure CNT, it can be observed that the doped CNT shows the enhancement of visible light absorption. The Si, B and N-doped CNT presents the overall optical absorption in the range of 300–800 nm, and the absorption center of Si, B and N-doped CNT locates at 409, 516 and 549 nm, respectively. Our result shows that the Si, B and N doping can promote the visible optical absorption of CNT and thus can enhance the visible light response. In addition, the Ni doped CNT also shows evident visible absorption. The absorption center of Ni-doped CNT locates at around 593 and 758 nm, and the absorption band edge shifts to the long wavelength region. According to these viewpoints, we can primarily conclude that the Si, Ni, B and N-doped CNTs are very promising visible photocatalytic materials.

4. Conclusions

We perform theoretical investigations of electronic structures, optical and structural properties of the pure CNT and Si, Ni, B and N-doped CNTs. The character of the properties exhibits dramatic variations depending on the type of a dopant atom. The bond distances and angles near the dopant Si and Ni atoms are severely distorted, however; dopant B and N atoms have small effects. The dopant Si, Ni, B and N atoms induce a decrase on the HOMO-LUMO gap and thus enhance the visible absorption of the pure CNT. The Si-doped CNT has the lowest HOMO-LUMO gap energy value thus the electronic transfer is easier. The optical refractive index values oscillate with based on a dopant atom on pure CNTs. B and N-doped models have the stronger intermolecular interaction due to larger

Table 2
Mulliken atomic charges of the pure CNT and Si, Ni, B and N-doped CNTs. C16 is a selected C atom in the pure CNT.

Atoms	CNT	Si-CNT	Ni-CNT	B-CNT	N-CNT
C1	−0.305304	−0.340681	−0.305982	−0.337489	−0.367082
C2	−0.304806	−0.348122	−0.366733	−0.353603	−0.362852
C3	−0.307605	−0.357877	−0.353377	−0.356075	−0.356820
C4	−0.303630	−0.346160	−0.361385	−0.339497	−0.362529
C5	−0.304367	−0.359593	−0.356484	−0.340681	−0.316612
C6	−0.306545	−0.291029	−0.344731	−0.310772	−0.270847
C7	0.066096	0.099122	0.139466	0.116153	0.125640
C8	0.066898	0.116911	0.111601	0.122739	0.110663
C9	0.065703	0.123909	0.152473	0.115257	0.089068
C10	0.065922	0.235304	0.111961	0.142329	0.188041
C11	0.066430	−0.312614	−0.147193	0.155276	0.113760
C12	0.066560	0.089335	0.102059	0.044164	0.127587
C13	0.066430	0.120659	0.128338	0.122095	0.117198
C14	0.066560	0.100747	0.111034	0.121415	0.166599
C15	0.066096	−0.327230	−0.210751	0.149131	0.025810
C16	0.066898	0.986272	0.734862	−0.141523	−0.294969
C17	0.065703	0.147464	0.051481	0.184087	0.176361
C18	0.065922	0.125991	0.099914	0.119003	0.117726
C19	−0.305304	−0.339990	−0.325904	−0.355328	−0.361960
C20	−0.304806	−0.300020	−0.341815	−0.355915	−0.282880
C21	−0.307605	−0.642245	−0.386324	−0.212957	−0.191727
C22	−0.303630	−0.322814	−0.361196	−0.384798	−0.320342
C23	−0.304367	−0.367537	−0.343931	−0.348374	−0.354125
C24	−0.306545	−0.352040	−0.355113	−0.345196	−0.355070
H25	0.239305	0.236851	0.239568	0.240466	0.232891
H26	0.238965	0.237669	0.240453	0.243069	0.234295
H27	0.239065	0.236382	0.236891	0.232340	0.236631
H28	0.239009	0.233794	0.232153	0.234963	0.232058
H29	0.239400	0.274665	0.229165	0.204397	0.243627
H30	0.238905	0.236112	0.227050	0.226042	0.238963
H31	0.239400	0.237550	0.238377	0.239225	0.234859
H32	0.238905	0.236493	0.239871	0.241947	0.236118
H33	0.239065	0.233651	0.230489	0.238787	0.236498
H34	0.239009	0.233695	0.236867	0.236141	0.235557
H35	0.239305	0.231132	0.236381	0.225719	0.237447
H36	0.238965	0.234245	0.230468	0.227464	0.240418

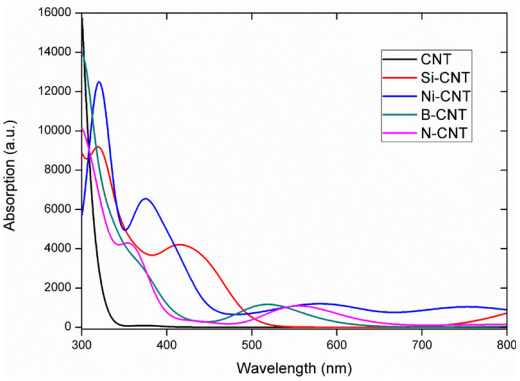

Fig. 7. Optical absorptions of the CNT and Si, Ni, B and N-doped CNTs.

dipole moment value. Dopant atom has significantly effect on the charge distributions on the atoms. From the formation energy analysis, the B and N doping on the pure CNT become more preferable in energy than Si and Ni-doped CNTs. The present work might be useful the understanding of the properties of doped-CNTs for the designing new nano electronic-devices.

Acknowledgment

This work was supported by the Ahi Evran University Scientific Research Projects Coordination Unit. Project Number: TBY.A4.18.004, TURKEY.

References

[1] T. Koretsune, S. Saito, J. Phys. Rev. B 77 (2008) 165417.
[2] W.-H. Chiang, G.-L. Chen, C.-Y. Hsieh, S.-C. Lo, RSC Adv. 5 (2015) 97579.
[3] J. Lu, X. Zhang, X. Wu, Z. Dai, J. Zhang, Sensors 15 (2015) 13522.
[4] B. Shan, K. Cho, Chem. Phys. Lett. 492 (2010) 131.
[5] K. Gong, F. Du, Z. Xia, M. Durstock, L. Dai, Science 323 (2009) 760.
[6] L. Qu, Y. Liu, J.B. Baek, L. Dai, ACS Nano 4 (2010) 1321.
[7] Z.Y. Zhang, K. Cho, Phys. Rev. B 75 (2007) 075420.
[8] G. Gao, S.H. Park, H.S. Kang, Chem. Phys. 355 (2009) 50.
[9] G.L. Guo, F. Wang, H. Sun, D.J. Zhang, Int. J. Quant. Chem. 108 (2008) 203.
[10] H.H. Jiang, D.J. Zhang, R.X. Wang, Nanotechnology 20 (2009) 145501.
[11] W. Kohn, L.J. Sham, Phys. Rev. 140 (1965) A1133.
[12] A.D. Becke, Phys. Rev. A 38 (1988) 3098.
[13] S.H. Vosko, L. Vilk, M. Nusair, Can. J. Phys. 58 (1980) 1200.
[14] C. Lee, W. Yang, R.G. Parr, Phys. Rev. B 37 (1988) 785.
[15] P.J. Hay, W.R. Wadt, J. Chem. Phys. 82 (1985) 270.
[16] W.R. Wadt, P.J. Hay, J. Chem. Phys. 82 (1985) 284.
[17] P.J. Hay, W.R. Wadt, J. Chem. Phys. 82 (1985) 299.
[18] M.J. Frisch, G.W. Trucks, H.B. Schlegel, G.E. Scuseria, M.A. Robb, J.R. Cheeseman, G. Scalmani, V. Barone, B. Mennucci, G.A. Petersson, et al., Gaussian 09, Revision B.01, Gaussian, Inc, Wallingford CT, 2009.
[19] Y. Li, R. Ahuja, J.A. Larsson, J. Chem. Phys. 140 (9) (2014) 091102.
[20] T. Yanai, D.P. Tew, N.C. Handy, Chem. Pys. Lett. 393 (2004) 51.
[21] M.E. Foster, B.M. Wong, J. Chem. Theory Comput. 8 (2012) 2682.
[22] A.P. Basile, F.E. Curchod, Alberto Fabrizio, L. Floryan, C. Corminboeuf, J. Phys. Chem. Lett. 6 (1) (2015) 13.
[23] E. Tanış, E.B. Şaş, M. Kurban, M. Kurt, J. Mol. Struct. 1154 (2018) 301.
[24] N.M. Ravindra, S. Auluck, V.K. Srivastava, Phys. Status Solidi B 93 (1979) K155.
[25] M. Kurban, B. Gündüz, J. Mol. Struct. 1137 (2017) 403.